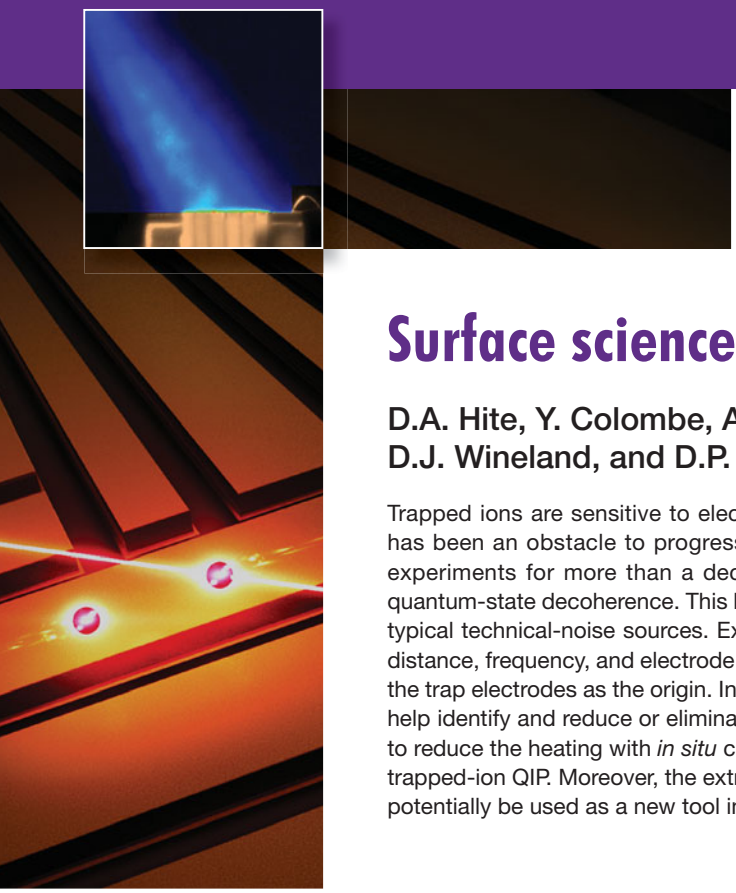


Surface science for improved ion traps

D.A. Hite, Y. Colombe, A.C. Wilson, D.T.C. Allcock, D. Leibfried, D.J. Wineland, and D.P. Pappas

Trapped ions are sensitive to electric-field noise from trap-electrode surfaces. This noise has been an obstacle to progress in trapped-ion quantum information processing (QIP) experiments for more than a decade. It causes motional heating of the ions, and thus quantum-state decoherence. This heating is anomalous because it is not easily explained by typical technical-noise sources. Experimental evidence of its dependence on ion-electrode distance, frequency, and electrode temperature points to the surface, rather than the bulk, of the trap electrodes as the origin. In this article, we review experimental efforts and models to help identify and reduce or eliminate the source of the anomalous heating. Recent progress to reduce the heating with *in situ* cleaning indicates that it may not be a fundamental limit to trapped-ion QIP. Moreover, the extreme sensitivity of trapped ions to electric-field noise may potentially be used as a new tool in surface science.

Introduction

Trapped atomic ions are used to explore the feasibility of quantum information processing (QIP) algorithms,[1–4] mainly aided by their inherent well-determined energy-level structure and relative isolation from the surrounding world. They have demonstrated all of the basic DiVincenzo criteria:[5] ability to initialize states of well-defined quantum bits (qubits), implementation of universal gate sets, long coherence times relative to gate durations, qubit specific readout, and scalability. Therefore, they are promising candidates for physical qubits to be used in QIP. However, as the scalability requirement motivates greater miniaturization with ions confined closer to the trap-electrode surfaces (**Figure 1**), the importance of interactions between ions and the trap electrodes grows.

Ideally, trapped ions only feel the force associated with an applied harmonic potential well and their mutual Coulomb repulsion. The applied potentials produce three-dimensional confinement, where the three motional modes for a single trapped ion typically have frequencies ranging from 0.1 MHz to 10 MHz. Multiple ions in the trap strongly repel each other, leading to a collective mode structure with $3N$ modes for N trapped ions. These modes are ideally laser-cooled to the ground state of motion, preparing a well-defined initial state for quantum logic operations that rely on Coulomb coupling between nearby qubit ions. In practice, however, the motion of the ions may be perturbed by stray electric fields from the environment, causing their quantum states to decohere. Even one quantum of motion absorbed from the environment during a two-qubit logic gate will ruin the fidelity of this operation.

In the context of quantum logic operations with ions, decoherence of the ions' motion refers mainly to the process whereby the initial and final motional-state wave functions in a two-qubit gate do not overlap. Many sources of motional decoherence have been identified. These include trap frequency instability, radiative heating such as that caused by Johnson noise (thermal electronic noise) from resistive elements, external electronic noise, field emission, and collisions with background gases.[6] In this article, we review efforts to understand and eliminate another noise source that has been a particular nuisance for trapped-ion QIP; that is, heating of the motional modes of ions (effectively, excitation of phonons in a collection of ions) from electric-field fluctuations originating from the surface of the trap electrodes. This is commonly referred to as anomalous heating, because the origin cannot be easily explained by any of the more obvious sources listed previously.

D.A. Hite, National Institute of Standards and Technology, Colorado; dustin.hite@nist.gov
Y. Colombe, National Institute of Standards and Technology, Colorado; yves.colombe@nist.gov
A.C. Wilson, National Institute of Standards and Technology, Colorado; andrew.wilson@nist.gov
D.T.C. Allcock, National Institute of Standards and Technology, Colorado; david.allcock@nist.gov
D. Leibfried, National Institute of Standards and Technology, Colorado; dietrich.leibfried@nist.gov
D.J. Wineland, National Institute of Standards and Technology, Colorado; david.wineland@nist.gov
D.P. Pappas, National Institute of Standards and Technology, Colorado; david.pappas@nist.gov
DOI: 10.1557/mrs.2013.207

© 2013 Materials Research Society
https://doi.org/10.1557/mrs.2013.207 Published online by Cambridge University Press

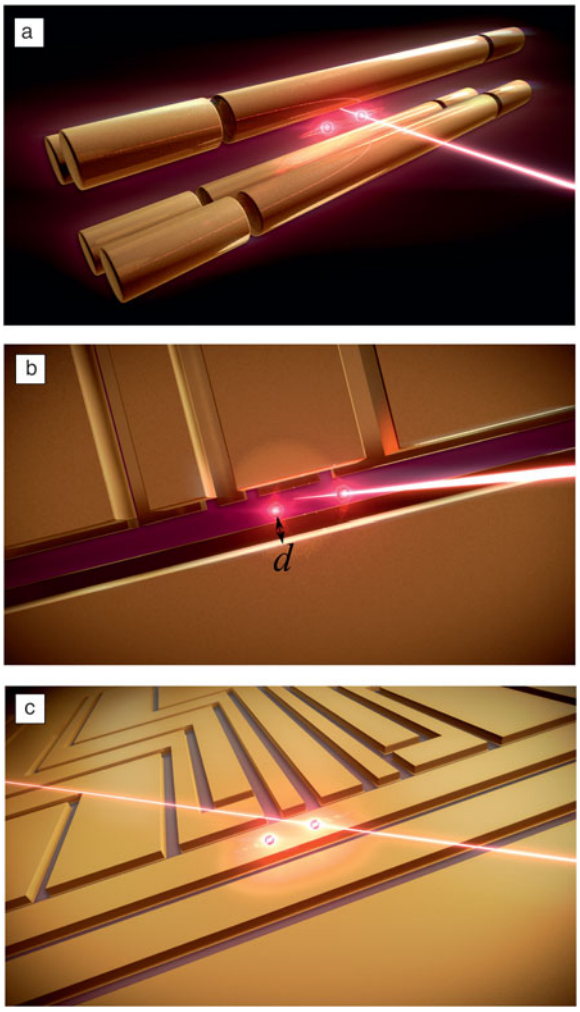


Figure 1. Illustration of various ion-trap geometries. The distance to the nearest electrode, *d*, is an important trap parameter. As *d* becomes smaller, motivated by scalability and faster quantum gates, electric-field noise above the electrodes increasingly heats the motion of the ions. (a) A simplified view of a quadrupole trap (adapted from Reference 6), which confines ions with a combination of rf and static electric fields. (b) The segmented-electrode linear ion trap used in Reference 32 has an ion-electrode distance, *d*, of ~140 μm. (c) Surface-electrode traps employ micro-fabricated electrodes on a substrate surface. In the surface-electrode trap shown here,[40,48] *d* = 40 μm. In Reference 71, *d* = 30 μm. Note that in these renderings, the ion-ion spacing may not be to scale.

Anomalous heating presents a major obstacle to continued progress in scalable trapped-ion QIP.

With accumulating data pointing to surface processes as the culprit, integration of ion traps with surface analysis and modification tools is warranted. For many reasons, this brings about a beneficial synergy between surface science and ion trapping. Since trapped-ion experiments are conducted in ultrahigh vacuum (UHV), the requisite environments for surface science and ion traps are compatible. In addition, the interface of interest in this case (i.e., the trap-electrode surface) is accessible to the *in situ* tools of surface science. Finally, since trapped ions are sensitive to nearby surfaces, a detailed understanding of the exact origin of anomalous heating could potentially turn the detection of ion heating into a new probe to study surface dynamical processes.

Anomalous motional heating of trapped ions: Physical models

Typical ion-ion spacing (often ~2–10 μm) renders any direct internal-state coupling (e.g., via dipole-dipole interactions) between qubits impractically weak for QIP. The key idea of Ignacio Cirac and Peter Zoller[1] was to use the long-range Coulomb interaction between ions, together with qubit state-dependent excitation of the ion motion, to execute two-qubit operations that can entangle the qubit states of two ions. This requires quantum coherence in the motion of the ions during the two-qubit gate operations. The motion of ions in the trapping potential, which can be described as harmonic-oscillator normal modes, must be well-isolated from the environment to maintain quantum coherence during a gate operation. Feasible quantum error correction demands that the energy in the harmonic oscillator, characterized by its average number of quanta, $\langle n \rangle$, should not increase by more than approximately 10^{-4} quanta during a gate operation.[7–9] For example, if the gate operation takes 10 μs, the heating rate, $d\langle n \rangle/dt$, should be less than 10 quanta/s. Thus, motional heating rates have become an important figure of merit in ion traps used for QIP.

Heating rates are typically determined by driving transitions that either add or subtract one quantum of motion. This process is asymmetric because no quantum can be subtracted if an ion is already in the ground state of motion. In that case, the probability, P_s, of a motion-subtracting transition vanishes, while the probability, P_a, of adding a quantum of motion is always finite. For a thermalized oscillator, we have $P_s/P_a = \langle n \rangle/\langle n+1 \rangle$. Heating rates can therefore be determined by comparing transition probabilities after preparing $\langle n \rangle < 1$ by laser cooling, then monitoring the growth of $\langle n \rangle$ as a function of the time after cooling. For an example of such a measurement, see **Figure 2**.

An obvious lower limit to the heating rate is due to thermal Johnson noise, where the potential of a conducting metal electrode fluctuates due to the thermal motion of electrons within the bulk of the metal. It came as a surprise that heating rates observed in experiments were often orders of magnitude higher than that expected from Johnson noise. Heating is driven by electric-field noise with spectral density $S_E(f)$ (expressed in units of $(V/m)^2/Hz$) that couples to the overall charge of the ions. This noise is sampled at the motional frequencies of the ions, where the harmonic motion constitutes a high-quality resonant system with very narrow intrinsic bandwidth. In this article, we focus on two important characteristic parameters: the distance, *d*, of the ions to the nearest electrode surface (Figure 1) and the exponent, α, of the frequency scaling of the noise spectral density, $S_E(f) \sim 1/f^{\alpha}$ (**Figure 3**). We note that the use of *d* as the distance to the nearest electrode gives only a rough (but convenient) measure; specifically, one should integrate

https://doi.org/10.1557/mrs.2013.207 Published online by Cambridge University Press

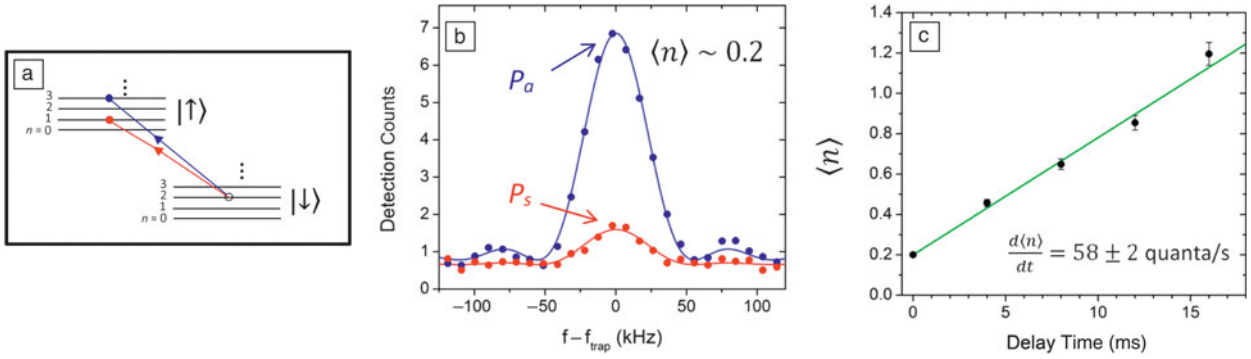


Figure 2. Basic elements of an example heating-rate measurement. (a) The $|\uparrow\rangle$ and $|\downarrow\rangle$ states denote the ion's internal qubit state, and the individual levels, denoted by n, represent the quantized states of a particular mode of motion in the trap. Motion-subtracting (red) and motion-adding (blue) transitions are used to determine the mean quantum number of the motional mode, which is in a thermal state. If an ion is prepared in the ground state of motion, the probability, P_s, to make a motion-subtracting transition vanishes, while the probability, P_a, of a motion-adding transition remains non-zero. Adapted from Reference 6. (b) By measuring the ratio $P_s/P_a = \langle n\rangle/\langle n+1\rangle$, the average motional state $\langle n\rangle$ can be determined (data from study in Reference 48). (c) Heating rates are then measured from the time rate of change of $\langle n\rangle$ over increasing delay times. Reprinted with permission from Reference 48. © 2012 American Physical Society.

over the entire electrode geometry to determine an effective value of d.

In early experiments, it became clear that the scaling of $S_E(f)$ with the ion-electrode distance, d, was stronger than $1/d^2$, as expected from Johnson noise arising from electrode resistance or resistors attached to the electrodes. Observations seemed to indicate the opposite limit, where the noise can be thought of as emanating from patches on the electrode surface that are much smaller than d. In this case, one can neglect the exact details of the sources, as their far-field always appears as that of an independent ensemble of electric dipoles. For dipoles, the electric-far-field drops as $1/d^3$, and therefore $s_E(f)$ for a single patch scales as $1/d^6$. Roughly speaking, the ion is sensitive to patches in an area proportional to d^2; therefore, if the noise of all patches in this area is incoherently summed, $S_E(f) = \sum s_E(f)$ should be proportional to $d^2/d^6 = 1/d^4$. More detailed calculations confirm this conclusion.[10–12]

Johnson noise creates voltage fluctuations that are intrinsically independent of frequency. If the applied electrode potentials are low-pass filtered (which is usually the case), $S_E(f)$ should scale as $1/f^2$ (i.e., $\alpha = 2$) for frequencies higher than the cutoff, depicted in Figure 3a. Using the effective resistance of a Thévenin equivalent circuit, which accounts for all elements in the filtered trap electrodes, one can simulate the electric-field noise spectral density from the Johnson voltage noise in the circuits. These estimates are often orders of magnitude lower than the electric-field noise observed in ion traps. Moreover, the frequency scaling of $S_E(f)$ in real traps often has been found to scale with $\alpha < 2$.[10] These discrepancies made materials and processing techniques used to fabricate trap electrodes a prime suspect in anomalous heating.[10,13,14]

It was suggested[6] that patch effects from surface dynamical processes of adsorbates may be responsible for the high-frequency electric-field noise perturbing the motion of the ions. Patch effects from adsorbate contamination on electrode surfaces have been studied extensively in vacuum electronic devices employing field-emission, secondary-emission, and photo-emission currents.[15] They arise from variations in the local work function due to patches of variable surface composition, giving rise to surface contact potentials. As elucidated in field-emission current flicker-noise studies, surface diffusion of adatoms, depicted in Figure 3b, is responsible for a frequency-dependent electron-current noise spectral density.[16–18] Analysis by Gesley and Swanson[19] confirmed a $1/f^{3/2}$ frequency dependence in the high frequency limit, previously measured by Timm and van der Ziel.[16] Additional structure in the frequency dependence is observed when one considers bounded versus unbounded diffusion with various probe/total area ratios.[20] The main features of such an adatom-diffusion noise model are $1/d^4$ distance scaling, direct dependence on adatom concentration and temperature, and a $\alpha = 3/2$ frequency dependence.

Alternative models have been put forth concerning electric-field noise from fluctuating electric dipoles of adsorbates to explain anomalous heating in ion traps.[11,21] These models, which also predict a $1/d^4$ distance scaling, detail how surface phonons mediate fluctuations in adatom dipole moments, causing electric-field noise above the surface (Figure 3c). Safavi-Naini et al.[11] used *ab initio* computations for the vibrational modes of adatoms adsorbed on an Au surface, and then calculated the resulting thermally excited dipole-moment noise spectral density. Relative to the fundamental phonon-induced transition rate, the predicted frequency scaling is flat (frequency-independent) for low frequencies, evolving to $1/f$, and then $1/f^2$ at even higher frequencies. Other phenomenological models based on fluctuating surface dipoles also may provide insight into the problem.[12] A complete study of the frequency and temperature dependence of electric-field noise from surfaces is needed to resolve the dominant mechanism.

Finally, charge traps in amorphous solids and at interfacial defect sites, in the form of microscopic two-level states

https://doi.org/10.1557/mrs.2013.207 Published online by Cambridge University Press

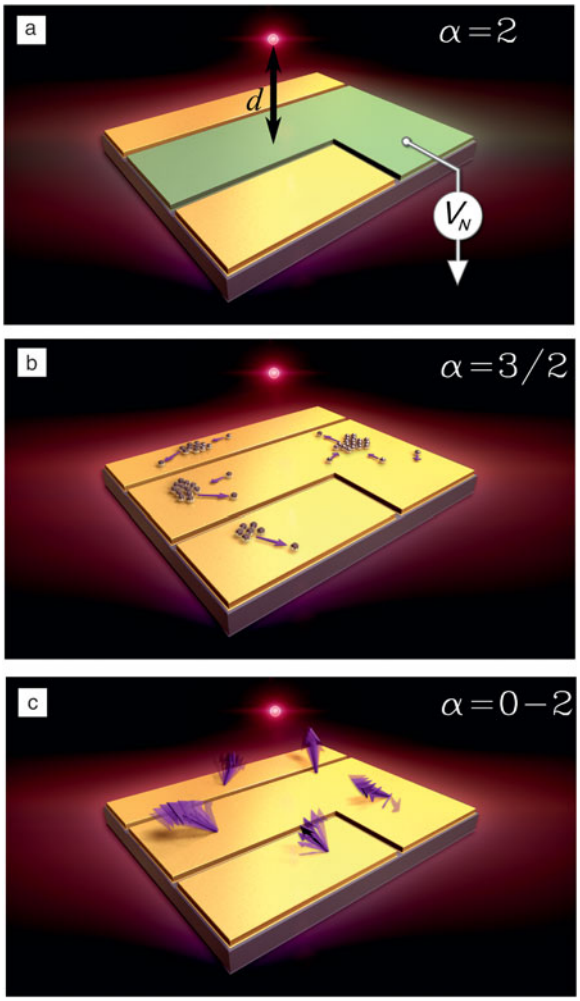


Figure 3. Depiction of various physical models of electric-field noise above ion-trap surfaces. Motional ion heating is driven by electric-field noise with spectral density $S_E \sim 1/f^{\alpha}$. (a) An entire electrode fluctuates due to Johnson noise (adapted from Reference 6) from resistance in external circuit elements (V_N), and thus S_E should scale as $\sim 1/d^2$ and $\alpha = 2$ (for frequencies higher than the low-pass filter cutoff). (b) Noise in the diffusion model is derived from local work-function fluctuations due to adsorbate surface diffusion. Work-function fluctuations are dependent on varying adsorbate concentrations. Spectral analysis[19] of adsorbate-concentration fluctuation predicts $\alpha = 3/2$. If contamination patches are small compared to the ion-electrode spacing, S_E from this model would scale as $\sim 1/d^4$. (c) In the dipole-fluctuation model, the dipole moments of adsorbed atoms (or molecules) fluctuate due to interactions with lattice vibrations in the electrode. In this model, S_E scales as $\sim 1/d^4$ and $\alpha = 1$ near the fundamental phonon-induced transition rate and evolves to $\alpha = 2$ at higher frequencies.[11]

thought to be responsible for noise in superconducting qubits,[22] may also play a role in anomalous heating. Localized electronic states can arise from Anderson localization (trapping of electron waves by interference in disordered solids) and give rise to a $1/f$-type noise spectral density in electron tunneling current.[23] Localized electronic states may also arise from defect states in ultra-thin dielectric overlayers on metal surfaces.[24] Therefore, the frequency dependence of electric-field noise measured in trapped-ion experiments can shed light on the responsible physical mechanism. For example, as Pendry et al. pointed out, diffusion of adatoms "can produce noise, but with a $1/f^{3/2}$ spectrum and should be distinguishable from the effects discussed here" (i.e., $(1/f)$-noise from charge traps).[23]

Experimental evidence for surface origins of noise

Over the past 15 years, many ion traps have been designed and implemented to investigate anomalous heating. Since the first demonstrations of ground-state cooling of trapped ions,[13,14] anomalously large heating rates have been observed. Turchette et al. measured motional heating from the ground state in traps of various sizes and electrode materials.[10] Their results were consistent with a small-patch model for electric-field noise from the surface of the trap electrodes. Since then, many groups around the world have constructed various rf (Paul) ion traps with different materials, ion-electrode distances, and electrode temperatures. While some traps have unique geometries for special purposes (i.e., for movable electrodes or enhanced optical access), most rf ion traps used for quantum information have the general geometric design of a linear trap, depicted in Figure 1a–b. To meet the scalability requirement, many ion traps are now micro-fabricated, making use of standard lithographic techniques, to confine the ion above a trap chip, depicted in Figure 1c. In these surface-electrode traps,[25] ions are routinely trapped at distances less than 100 μm from the electrode surface. Since anomalous heating scales inversely with the ion-electrode distance d, surface-electrode traps have provided a wealth of data on this distance dependence (included in **Figure 4**).

Early on, materials for trap electrodes were chosen for their bulk physical properties, for example, molybdenum electrodes[10,13,14] were used for their electrical, non-magnetic, and structural qualities, as well as static contact-potential stability. As ion trappers became aware of the possible surface origins of anomalous heating, more noble, and some not-so-noble, materials were tested in traps, including Au, Ag, Al, W, Si, GaAs, Nb, and NbN, among others (see references in Figure 4). An important practical problem in the search for the best materials is the significant time required to design, fabricate, clean, assemble, and vacuum process the trap structure, and then measure heating rates as a function of electrode material. One approach to solve this materials-testing problem is the implementation of a stylus-type ion trap, suggested by Maiwald et al., to characterize various surfaces brought into close proximity to a trapped ion.[26] However, at present, all available data are from complete, fabricated traps.

Deposition of neutral atoms (typically Be, Mg, Ca, Sr, Ba, Hg, Cd, or Yb used for qubit ions) that occurs during the trap loading process has also been cited as a source of increased motional heating over time.[10,12,27] Presumably, patch effects from changing work functions cause stray fields

https://doi.org/10.1557/mrs.2013.207 Published online by Cambridge University Press

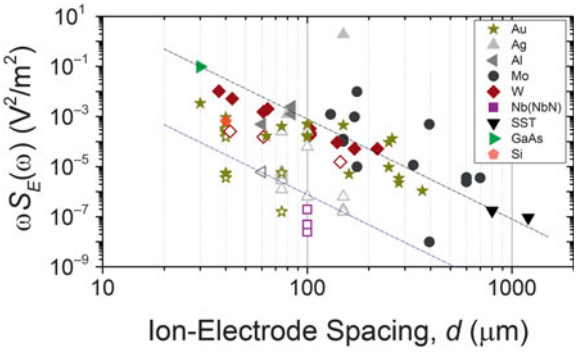


Figure 4. Normalized electric-field noise spectral density versus ion-electrode distance, d. Since electric-field noise in ion traps scales approximately with $1/f$, we normalize by the frequency $\omega = 2\pi f$ to compensate for this effect. The symbols distinguish traps fabricated with different electrode materials. The dash-dotted lines indicate a $1/d^4$ scaling predicted by small-patch noise models and are plotted as an aid to guide the eye (vertical position not relevant). These electric-field noise data seem to be independent of electrode material. Open symbols represent data employing cryogenic electrodes, indicating the thermally activated nature of the noise source (Au,[10,12,25,38,40,48,64,66,69–71] Ag,[37] Al,[28,53] Mo,[10,13,14,62,63] W,[36] Nb,[39] stainless steel (SST),[67,68] GaAs,[65] Si[29]).

to vary locally. This can be exacerbated by a photoionization laser used to create the ions near the trap surface in a region of high rf fields. The deposition kinetics for these conditions have not been well studied; however, many technical solutions have been implemented, namely back-side loading,[28–31] use of a separate load zone and shuttling,[32,33] and even loading with a pre-cooled, neutral cloud manipulated in a magneto-optical trap.[34,35]

In an effort to corroborate Turchette's experimental results that indicated an ~ $1/d^4$ ion-electrode distance scaling (consistent with the small-patch model), Deslauriers et al. constructed a "needle" trap with moveable tungsten electrodes.[36] In their apparatus, they were able to measure ion heating rates with an ion-electrode distance ranging from ~40 to 200 μm with the same electrodes (see diamond symbols in Figure 4). Their results indicated a distance dependence of $1/d^{3.5\pm0.1}$. While this is not exactly $1/d^4$, the authors note that the electric-field noise from microscopic patches on the needle electrodes also depends on the details of the electrode geometry, but that their results certainly ruled out Johnson noise. Lending more evidence, the magnitude of the observed noise was two orders of magnitude higher than expected from Johnson-noise estimates. Moreover, the frequency-dependence measurement yielded a value of $\alpha = 0.8 \pm 0.2$ for the electric-field noise spectral density. The needle trap was also equipped with the ability to cool the electrodes to ~150 K with liquid nitrogen, resulting in a reduction in the ion heating rate by an order of magnitude. This was the first experimental indication that the mechanism for anomalous heating is a thermally activated process. This also ruled out Johnson noise, since it did not scale linearly with temperature.

Labaziewicz et al. demonstrated further improvements by operating surface-electrode traps at temperatures as low as 6 K.[37,38] Operation at such low temperature also led to the demonstration of a micro-fabricated ion trap with superconducting electrodes.[39] Since the heating rate did not change appreciably when the trap was operated above and below T_c, this work confirmed that anomalous heating is not due to bulk resistivity and provides further evidence that the noise sources originate at the electrode surfaces. Although significantly reduced, the observed electric-field noise at cryogenic temperatures remains substantially larger than estimates based on Johnson noise. In addition, large and variable values in the observed electric-field noise (Figure 4) highlight the fact that the source persists independent of the methods used to fabricate the traps.

While various electrode materials have been tested in cryogenic surface-electrode traps,[28,37–40] to date, most employ Au electrodes because of its apparent nobility.[41] However, there are some exceptions to this line of thought. First, it is important to note that the ideal surface might be one that exhibits a uniform work function at least over the area sensed by the ion. However, the work function of bare metal surfaces varies significantly depending on the crystallographic orientation, roughness, and step structure of the surface.[42,43] Since there is always some mobility of adatoms at the surface, fluctuations of the work function, and hence, the field sensed by the ion, can be expected. Second, and perhaps more importantly, the surface of the trap is exposed to a long chain of processing and heating steps over the course of assembly, typically culminating in the final vacuum bake of the system. In the specific case of the Au surface, this causes a thin layer of carbon contamination to accumulate (see **Figure 5**a). The carbon contamination is most likely caused by a combination of rough surface morphology[44] and activated hydrocarbons from the environment.[45–47] Because the final step in vacuum processing may be the ultimate surface contamination source, *in situ* surface preparation and modification may be a necessary step in ion-trap construction.

In situ cleaning of ion-trap surfaces

From a surface science point of view, all surfaces are contaminated until prepared *in situ* under UHV conditions. Examples of clean surface preparations include cleavage along a crystal plane, cycles of ion bombardment and annealing, flash annealing to desorb surface atoms, oxidation/reduction reactions, photo-induced desorption, and film growth/deposition. Even after cleaning *in situ*, the time before a surface is deemed contaminated again depends on the sticking coefficient of the surface of interest, the partial pressure of the contaminant species in the vacuum (or diffusion constant for migrating impurities from the bulk into a depleted region near the surface), and the sensitivity of the probe. As a conservative estimate, assuming a low sticking coefficient of 0.1 and a residual contaminant background gas partial pressure of ~10^{-9} Pa, a 0.1 monolayer contamination would be detected within about one day.

https://doi.org/10.1557/mrs.2013.207 Published online by Cambridge University Press

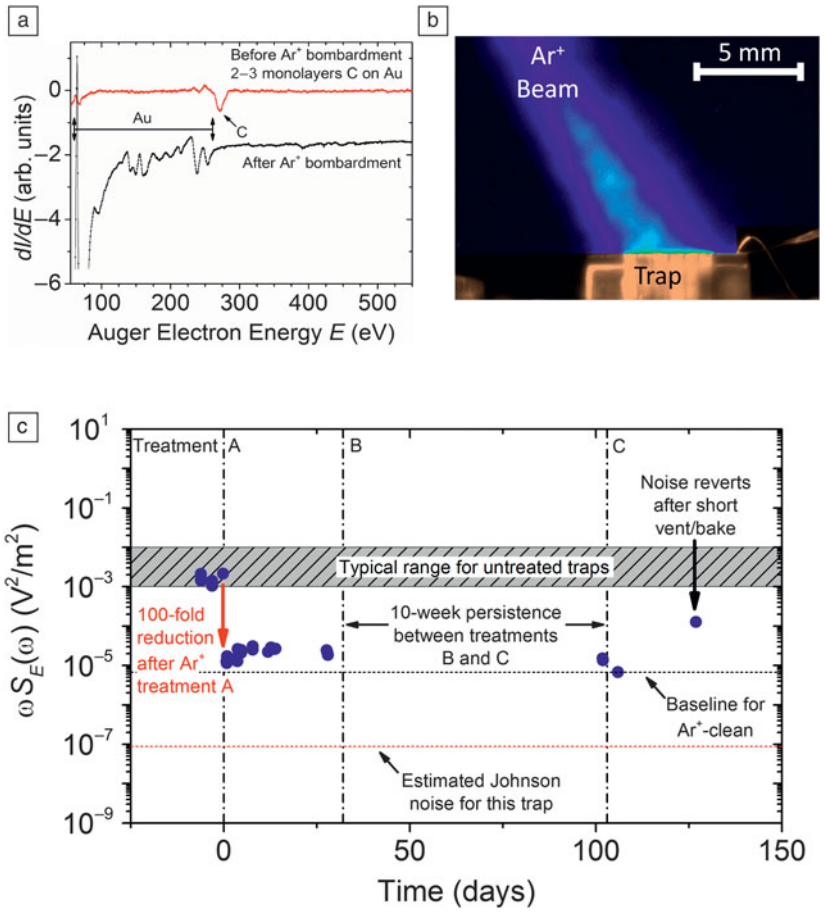


Figure 5. Surface analysis and modification used to reduce anomalous heating by two orders of magnitude. (a) Auger electron spectroscopy reveals oxygen-free carbonaceous overlayers on trap surfaces after fabrication and vacuum baking (red trace). The spectrum after Ar^+ bombardment (black trace), offset downward for clarity, shows only features that indicate an Au surface free of these contaminants. (b) Enhanced, false-color image of the surface-electrode trap in side view and Ar^+ beam used to clean the ion-trap surface *in situ*. (c) A 100-fold reduction in electric-field noise is observed after treating the trap with Ar^+ bombardment. These low levels of electric-field noise were observed to persist for several weeks. The lowest level achieved corresponds to a heating rate of ~43 quanta/s for a Be^+ ion at f = 3.6 MHz and d = 40 μm in a room-temperature trap. Each of the treatments (A, B, and C) have the same ion-bombardment parameters (2 kV, ~100 C/m², 5 × 10^{-3} Pa, ~45 min). Hatched area denotes range of electric-field noise for untreated, room-temperature traps with d ~40 μm. For comparison, (c) has the same vertical scale as Figure 4. Reprinted with permission from Reference 48. © 2012 American Physical Society.

Commonly, electron spectroscopy, such as Auger electron spectroscopy (AES) or x-ray photoelectron spectroscopy, is used to detect surface contaminants at ~1% of a monolayer level. In light of the evidence that anomalous heating in ion traps is a surface-related problem, the logical first step is to clean the surface *in situ*. In the remainder of this article, we review efforts to reduce anomalous heating in ion traps by use of *in situ* treatments to the trap electrode surfaces.

Recently, AES surface analysis of ion-trap electrodes, micro-fabricated from a 10-μm-thick electroplated Au film, *ex situ* cleaned with organic solvents, and then vacuum baked to ~470 K, revealed the presence of a 2–3 monolayer (ML) thick carbonaceous overlayer on the trap surface.[48] This is consistent with the residue from reactions of a gold surface and hydrocarbons present in the atmosphere. With use of argon-ion bombardment (2 kV, ~100 C/m², 5 × 10^{-3} Pa, ~45 min), these contaminant overlayers are easily removed, revealing a pristine Au surface, at least to the sensitivity level of AES (Figure 5a). However, *ex situ* transfer of these cleaned surfaces to a separate ion-trap chamber is precluded by at least two effects. First, when these cleaned surfaces are exposed to an atmosphere of dry nitrogen gas for ~ tens of minutes, they re-acquire ~0.5 ML of carbon, presumably from impurities.[46] Second, even a clean Au surface re-acquires ~2–3 ML of carbon after baking, presumably from desorption from the chamber walls. It is important to note, however, that in UHV, argon-cleaned Au surfaces remain clean for several weeks. Other cleaning techniques such as a reactive plasma discharge[47] or UV/ozone[49] may be effective in cleaning trap surfaces; however, recovery of UHV conditions may be difficult after the high pressure (>1 Pa) gas load required for these treatments.

Surface cleaning and adsorbate removal through the application of high-intensity laser pulses has been established as an effective technique in many studies.[50] Though not as widely used as ion bombardment, thermal annealing, or plasma cleaning, it has some definite practical advantages for trapped-ion experiments. Foremost among these is the fact that it can be done under UHV conditions without the need to introduce a process gas, a particular advantage in cryogenic systems. Experimental complexity is further reduced by the fact that no extra hardware is required inside the vacuum system, which can also limit optical access. Furthermore, laser cleaning can be applied selectively to small areas of the trap and from any direction in which there is optical access, an advantage when cleaning complex 3D trap structures.

There are two distinct regimes for pulsed-laser cleaning: the long pulse regime (longer than a few picoseconds) and the ultrafast regime (sub-picosecond). In the long pulse regime, the predominant process is thermal heating of the metal surface (to a depth of tens of micrometers for a few-nanosecond pulse), which leads to desorption and, at high enough energies, melting.[51] UV wavelengths are preferred for removing organics, as they typically absorb strongly at these wavelengths.[52] A recent experiment employed 3–5-ns pulses from a frequency-tripled Nd:YAG laser at 355 nm to clean an ion-trap surface *in situ*.[53] This resulted in a decrease in the ion heating rate by a factor of 2. In the ultrafast regime, thermal propagation is negligible, and instead, a thin surface layer (tens of nanometers)

https://doi.org/10.1557/mrs.2013.207 Published online by Cambridge University Press

ionizes to form a plasma. It has been shown that this causes minimal thermal and mechanical disruption to the underlying material,[54] and thus may be a promising avenue for future study.

In another recent trapped-ion heating-rate study, *in situ* argon ion bombardment was implemented in a room-temperature ion-trap apparatus.[48] In this study, an electroplated Au surface-electrode trap, whose fabrication was the same as the test surfaces studied with AES, shown in Figure 5a, was used to investigate the frequency dependence of electric-field noise in the trap before and after ion bombardment and after subsequent venting and re-baking of the vacuum chamber. As shown in Figure 5c, before an Ar^+ beam cleaning treatment, the heating rate of the trap was similar to other surface-electrode traps (~16,000 quanta/s, $d = 40$ μm, $f = 3.6$ MHz, Be^+). A 100-fold reduction in the heating rate was observed after a cleaning treatment to a value (~100 quanta/s) that compares favorably with traps operated at 4 K. The substantially reduced heating rate was observed to persist for 10 weeks, before the trap surface was intentionally exposed to air (Figure 5c). After re-baking the system with the cleaned trap chip, heating rates were observed to revert back to the typical high values commonly seen in untreated ion traps. Re-cleaning with the Ar^+ beam again reduced the heating rate. This provides compelling evidence that the origin of anomalous heating is from adsorbate-related processes on the electrode surfaces, and the ion can be thought of as a sensor for such phenomena.[55]

As noted previously, the frequency dependence of the electric-field noise spectral density may aid in determining the responsible physical mechanisms. In Reference 48, the frequency exponent, α, was measured before and after the cleaning treatment to be 1.53 ± 0.07 and 1.57 ± 0.04, respectively. On one hand, this value is consistent with the adatom-diffusion model described previously, where the theory gives $\alpha = 3/2$. If work-function fluctuations due to adatom diffusion is the principal mechanism for anomalous heating, even at low temperatures, α would remain to be 3/2, although the magnitude of S_E would be reduced. On the other hand, the dipole-fluctuation model can account for these measurements only under a narrow range of parameters, and the frequency scaling would change as a function of temperature.[11] Therefore, measurement of α at low temperature over the same frequency range as room temperature could help determine which model holds.

The fact that α was measured to be the same before and after the cleaning treatment is an indication that the physical noise mechanism is the same, albeit significantly reduced. This could be explained if the trapped ion is sensitive to the self-diffusion of Au adatoms on the clean surface. An alternative explanation is that the ion is sensitive to adsorbate-concentration levels below the detection threshold of common electron spectroscopy techniques such as AES. Since the role of surface morphology was not investigated in this work, these variables will need to be further studied. The electric-field noise from this trap remained two orders of magnitude higher than the Johnson-noise estimate, but there is hope that *in situ* cleaning of trap electrodes in combination with cryogenic cooling might sufficiently reduce anomalous heating to enable significantly improved quantum information experiments. The lowest observed heating rate of $d\langle n\rangle/dt = 43$ quanta/s would imply an error probability of 4.3×10^{-4} for a 10 μs gate. Reducing the heating rate by another factor of 10 would allow for a regime where quantum error correction can come into play. Additional studies are required to elucidate the responsible mechanisms, and might, at the same time, expand our knowledge of surface processes into a previously unexplored domain.

Summary

Motional heating from electric-field noise in ion traps has been an obstacle to progress in trapped-ion QIP experiments for more than a decade. We have reviewed the experimental evidence that anomalous heating in ion traps originates from surface-related phenomena on the trap electrodes, rather than from bulk processes. Dependencies on ion-electrode distance, frequency scaling, electrode temperature, materials, far-from-equilibrium deposition of neutrals, superconductivity, and *in situ* surface-cleaning treatments provide strong evidence that thermal Johnson noise from bulk resistance is typically not the source of these electric-field fluctuations. *In situ* surface preparation and analysis appears to provide a promising way to reduce and study the heating.

Further experimentation and modeling are required to elucidate the exact origin of this electric-field noise; however, due to their resonant sensitivity to high-frequency electromagnetic fields, trapped ions may become a promising new tool to study surfaces. Finally, the work reviewed here may have significant relevance to other, closely related trapped-ion experiments, such as time and frequency standards and their applications,[56] and other fields, such as nanoelectromechanical resonators,[57] precision gravity measurements,[58] tests of general relativity,[59] and Casimir-force investigations,[60,61] where surface patch potentials have a strong influence.

Acknowledgments

This article is a contribution of NIST and is not subject to US copyright. This work was supported by IARPA under ARO Contract Numbers DNI-017389 and EAO-139840, ONR, and the NIST Quantum Information Program. We thank Jim Bergquist, Jim Phillips, and Mark Gesley for helpful discussions, and K.S. McKay and M.R. Vissers for suggestions on the manuscript.

References

1. J.I. Cirac, P. Zoller, *Phys. Rev. Lett.* **74**, 4091 (1995).
2. R. Blatt, D.J. Wineland, *Nature* **453**, 1008 (2008).
3. R. Blatt, C.F. Roos, *Nat. Phys.* **8**, 277 (2012).
4. C. Monroe, J. Kim, *Science* **339**, 1164 (2013).
5. D.P. DiVincenzo, *Fortschr. Phys.* **48**, 771 (2000).
6. D.J. Wineland, C. Monroe, W.M. Itano, D. Leibfried, B.E. King, D.M. Meekhof, *J. Res. Nat. Inst. Stand. Technol.* **103**, 259 (1998).
7. J. Preskill, *Proc. R. Soc. London, Ser. A* **454**, 385 (1998).
8. A. Sørensen, K. Mølmer, *Phys. Rev. A* **62**, 022311 (2000).
9. E. Knill, *Nature* **463**, 441 (2010).
10. Q.A. Turchette, D. Kielpinski, B.E. King, D. Leibfried, D.M. Meekhof, C.J. Myatt, M.A. Rowe, C.A. Sackett, C.S. Wood, W.M. Itano, C. Monroe, D.J. Wineland, *Phys. Rev. A.* **61** 063418 (2000).

https://doi.org/10.1557/mrs.2013.207 Published online by Cambridge University Press

11. A. Safavi-Naini, P. Rabl, P.F. Weck, H.R. Sadeghpour, *Phys. Rev. A* **84**, 023412 (2011).
12. N. Daniilidis, S. Narayanan, S.A. Möller, R. Clark, T.E. Lee, P.J. Leek, A. Wallraff, St. Schulz, F. Schmidt-Kaler, H. Häffner, *New J. Phys.* **13**, 013032 (2011).
13. F. Diedrich, J.C. Bergquist, W.M. Itano, D.J. Wineland, *Phys. Rev. Lett.* **62**, 403 (1989).
14. C. Monroe, D.M. Meekhof, B.E. King, W.M. Itano, D.J. Wineland, *Phys. Rev. Lett.* **75**, 4714 (1995).
15. A. van der Ziel, *Adv. Electron. El. Phys.* **49**, 225 (1979).
16. G.W. Timm, A. van der Ziel, *Physica* **32**, 1333 (1966).
17. Ch. Kleint, *Surf. Sci.* **200**, 472 (1988).
18. R. Gomer, *Rep. Prog. Phys.* **53**, 917 (1990).
19. M.A. Gesley, L.W. Swanson, *Phys. Rev. B* **32**, 7703 (1985).
20. M. Gesley, L. Swanson, *Phys. Rev. A* **37**, 4879 (1988).
21. A. Safavi-Naini, E. Kim, P.F. Weck, P. Rabl, H.R. Sadeghpour, *Phys. Rev. A* **87**, 023421 (2013).
22. L. Faoro, L.B. Ioffe, *Phys. Rev. Lett.* **96**, 047001 (2006).
23. J.B. Pendry, P.D. Kirkman, E. Castano, *Phys. Rev. Lett.* **57**, 2983 (1986).
24. H.M. Benia, P. Myrach, A. Gonchar, T. Risse, N. Nilius, H.J. Freund, *Phys. Rev. B* **81**, 241415 (2010).
25. S. Seidelin, J. Chiaverini, R. Reichle, J.J. Bollinger, D. Leibfried, J. Britton, J.H. Wesenberg, R.B. Blakestad, R.J. Epstein, D.B. Hume, W.M. Itano, J.D. Jost, C. Langer, R. Ozeri, N. Shiga, D.J. Wineland, *Phys. Rev. Lett.* **96**, 253003 (2006).
26. R. Maiwald, D. Leibfried, J. Britton, J.C. Bergquist, G. Leuchs, D.J. Wineland, *Nat. Phys.* **5**, 551 (2009); C.L. Arrington et al., *Rev. Sci. Instrum.* **84**, 085001 (2013).
27. R. DeVoe, C. Kurtsiefer, *Phys. Rev. A* **65**, 063407 (2002).
28. D.R. Leibrandt, J. Labaziewicz, R.J. Clark, I.L. Chuang, R.J. Epstein, C. Ospelkaus, J.H. Wesenberg, J.H. Bollinger, D. Leibfried, D. Wineland, D. Stick, J. Sterk, C. Monroe, C.-S. Pai, Y. Low, R. Frahm, R.E. Slusher, *Quantum Inf. Comput.* **9**, 901 (2009).
29. J. Britton, D. Leibfried, J.A. Beall, R.B. Blakestad, J.H. Wesenberg, D.J. Wineland, *Appl. Phys. Lett.* **95**, 173102 (2009).
30. D. Stick, K.M. Fortier, R. Haltli, C. Highstrete, D.L. Moehring, C. Tigges, M.G. Blain, *Physics* (2010) (available at http://arxiv.org/abs/1008.0990v2).
31. J.T. Merrill, C. Volin, D. Landgren, J.M. Amini, K. Wright, S.C. Doret, C.-S. Pai, H. Hayden, T. Killian, D. Faircloth, K.R. Brown, A.W. Harter, R.E. Slusher, *New J. Phys.* **13**, 103005 (2011).
32. M.D. Barrett, J. Chiaverini, T. Schaetz, J. Britton, W.M. Itano, J.D. Jost, E. Knill, C. Langer, D. Leibfried, R. Ozeri, D.J. Wineland, *Nature* **429**, 737 (2004).
33. R.B. Blakestad, C. Ospelkaus, A.P. VanDevender, J.H. Wesenberg, M.J. Biercuk, D. Leibfried, D.J. Wineland, *Phys. Rev. A* **84**, 032314 (2011).
34. M. Cetina A. Grier, J. Campbell, I. Chuang, V. Vuletic, *Phys. Rev. A* **76**, 041401 (2007).
35. J.M. Sage, A.J. Kerman, J. Chiaverini, *Phys. Rev. A* **86**, 013417 (2012).
36. L. Deslauriers, S. Olmschenk, D. Stick, W.K. Hensinger, J. Sterk, C. Monroe *Phys. Rev. Lett.* **97**, 103007 (2006).
37. J. Labaziewicz Y.F. Ge, P. Antoli, D. Leibrandt, K.R. Brown, I.L. Chuang, *Phys. Rev. Lett.* **100**, 013001 (2008).
38. J. Labaziewicz, Y.F. Ge, D. Leibrandt, S.X. Wang, R. Shewmon, I.L. Chuang, *Phys. Rev. Lett.* **101**, 180602 (2008).
39. S.X. Wang, Y.F. Ge, J. Labaziewicz, E. Dauler, K. Berggren, I.L. Chuang, *Appl. Phys. Lett.* **97**, 244102 (2010).
40. K.R. Brown, C. Ospelkaus, Y. Colombe, A.C. Wilson, D. Leibfried, D.J. Wineland, *Nature* **471**, 196 (2011).
41. B. Hammer, J.K. Nørskov, *Nature* **376**, 238 (1995).
42. G.V. Hansson, S.A. Flodström, *Phys. Rev. B* **18**, 1572 (1978).
43. T.-S. Lin, Y.-W. Chung, *Superlattices Microstruct.* **4**, 709 (1988).
44. M. Chaigneau, G. Picardi, R. Ossikovski, *Surf. Sci.* **604**, 701 (2010).
45. K. Boller, R.P. Haelbich, H. Hogrefe, W. Jark, C. Kunz, *Nucl. Instrum. Methods* **208**, 273 (1983).
46. J. Krim, *Thin Solid Films* **137**, 297 (1986).
47. R.E. Clausing, L.C. Emerson, L. Heatherly, R.J. Colchin, J.C. Twichell, *J. Vac. Sci. Technol.* **13**, 437 (1976).
48. D.A. Hite, Y. Colombe, A.C. Wilson, K.R. Brown, U. Warring, R. Jördens, J.D. Jost, K.S. McKay, D.P. Pappas, D. Leibfried, D.J. Wineland, *Phys. Rev. Lett.* **109**, 103001 (2012).
49. A. Krozer, M. Rodahl, *J. Vac. Sci. Technol., A* **15**, 1704 (1997).
50. Ph. Delaporte, R. Oltra, in *Recent Advances in Laser Processing of Materials (European Materials Research Society Series)*, J. Perriere, E. Millon, E. Fogarassy, Eds. (Elsevier, Amsterdam, 2006), pp. 411–440.
51. R. Viswanathan, I. Hussia, *J. Opt. Soc. B* **3**, 796 (1986).
52. H.K. Park, C.P. Grigoropoulos, W.P. Leung, A.C. Tam, *IEEE Trans. Compon. Packag. Manuf. Technol. Part A* **17**, 631 (1994).
53. D.T.C. Allcock, L. Guidoni, T.P. Harty, C.J. Ballance, M.G. Blain, A.M. Steane, D.M. Lucas, *New J. Phys.* **13**, 123023 (2011).
54. W. Kautek, J. Krüger, *Proc. SPIE* **2207**, 600 (1994).
55. After submission of this article, similar analyses and results have been reported by N. Daniilidis, S. Gerber, G. Bolloten, M. Ramm, A. Ransford, E. Ulin-Avila, I. Talukdar, H. Häffner, *Physics* (2013) (available at arXiv 1307.7194v1).
56. T. Rosenband, D.B. Hume, P.O. Schmidt, C.W. Chou, A. Brusch, L. Lorini, W.H. Oskay, R.E. Drullinger, T.M. Fortier, J.E. Stalnaker, S.A. Diddams, W.C. Swann, N.R. Newbury, W.M. Itano, D.J. Wineland, J.C. Bergquist, *Science* **319**, 1808 (2008).
57. Y.T. Yang, C. Callegari, X.L. Feng, M.L. Roukes, *Nano Lett.* **11**, 1753 (2011).
58. N.A Robertson, J.R. Blackwood, S. Buchman, R.L. Byer, J. Camp, D. Gill, J. Hanson, S. Williams, P. Zhou, *Class. Quantum Grav.* **23**, 2665 (2006).
59. R.D. Reasenberg, B.R. Patla, J.D. Phillips, R. Thapa, *Class. Quantum Grav.* **29**, 184013 (2012).
60. A.O. Sushkov, W.J. Kim, D.A.R. Dalvit, S.K. Lamoreaux, *Nat. Phys.* **7**, 230 (2011).
61. R.O. Behunin, Y. Zeng, D.A.R. Dalvit, S. Reynaud, *Phys. Rev. A* **86**, 052509 (2012).
62. Ch. Roos, Th. Zeiger, H. Rohde, H.C. Nägerl, J. Eschner, D. Leibfried, F. Schmidt-Kaler, R. Blatt, *Phys. Rev. Lett.* **83**, 4713 (1999).
63. Chr. Tamm, D. Engelke, V. Bühner, *Phys. Rev. A* **61**, 053405 (2000).
64. L. Deslauriers, P.C. Haljan, P.J. Lee, K.-A. Brickman, B.B. Blinov, M.J. Madsen, C. Monroe, *Phys. Rev. A* **70**, 043408 (2004).
65. D. Stick, W.K. Hensinger, S. Olmschenk, M.J. Madsen, K. Schwab, C. Monroe, *Nat. Phys.* **2**, 36 (2006).
66. R.J. Epstein, S. Seidelin, D. Leibfried, J.H. Wesenberg, J.J. Bollinger, J.M. Amini, R.B. Blakestad, J. Britton, J.P. Home, W.M. Itano, J.D. Jost, E. Knill, C. Langer, R. Ozeri, N. Shiga, D.J. Wineland, *Phys. Rev. A* **76**, 033411 (2007).
67. D.M. Lucas, B.C. Keitch, J.P. Home, G. Imreh, M.J. McDonnell, D.N. Stacey, D.J. Szwer, A.M. Steane, *Quantum Phys.* (2007) (available at arxiv/pdf/0710/0710.4421v1.pdf).
68. J. Benhelm, G. Kirchmair, C.F. Roos, R. Blatt, *Phys. Rev. A* **77**, 062306 (2008).
69. S.A. Schulz, U. Poschinger, F. Ziesel, F. Schmidt-Kaler, *New J. Phys.* **10**, 045007 (2008).
70. D.T.C. Allcock, J.A. Sherman, M.J. Curtis, G. Imreh, A.H. Burrell, D.J. Szwer, D.N. Stacey, A.M. Steane, D.M. Lucas, *New J. Phys.* **12**, 053026 (2010).
71. U. Warring, C. Ospelkaus, Y. Colombe, K.R. Brown, J.M. Amini, M. Carsjens, D. Leibfried, D.J. Wineland, *Phys. Rev. A* **87**, 013437 (2013). □

MRS OnDemand®
WEBINAR SERIES

The Materials Research Society® is excited to introduce the new **MRS OnDemand Webinar Series.** The program offers free, live webinars throughout the year, providing valuable educational information on timely, interdisciplinary topics.

NOW ACCEPTING WEBINAR PROPOSALS

Visit www.mrs.org/on-demand-webinars today to see a list of sponsor benefits and download the proposal submittal form.

VIEW THE FIRST IN THE SERIES
archived from June 11, 2013

Nanoindentation: Fundamentals and Frontiers
OnDemand now at **www.mrs.org/on-demand-webinars.**

George Pharr The University of Tennessee and Oak Ridge National Laboratory

Warren Oliver Nanomechanics, Inc.

https://doi.org/10.1557/mrs.2013.207 Published online by Cambridge University Press